2007-07

Design and Control of Libration Point Spacecraft Formations

Infeld, Samantha I.; Josselyn, Scott B.; Murray, Walter; Ross, Michael I.

The American Institute of Aeronautics and Astronautics (AIAA)

Infeld, Samantha I., et al. "Design and control of libration point spacecraft formations." Journal of Guidance, Control, and Dynamics 30.4 (2007): 899-909. http://hdl.handle.net/10945/66379

JOURNAL OF GUIDANCE, CONTROL, AND DYNAMICS
Vol. 30, No. 4, July–August 2007

Design and Control of Libration Point Spacecraft Formations

Samantha I. Infeld*
Stanford University, Stanford, California 94305-4035
Scott B. Josselyn†
Naval Postgraduate School, Monterey, California 39343
Walter Murray‡
Stanford University, Stanford, California 94305-4035
and
I. Michael Ross§
Naval Postgraduate School, Monterey, California 39343

DOI: 10.2514/1.18654

We investigate the concurrent problem of orbit design and formation control around a libration point. Concurrency implies that the design and control problem are simultaneously investigated. Separating the two problems is both unnecessary and ill-advised. The full problem can be naturally cast as a multi-agent, nonlinear, constrained optimal control problem. The optimality criterion is fuel consumption because the engineering feasibility of a formation design is dominated by the amount of propellant required to maintain a formation. Contrary to popular belief, quadratic costs do not measure fuel consumption; consequently, we take a direct measure of fuel consumption given by the L^1 norm of the control acceleration. Fuel budgets to individual spacecraft are allocated by isoperimetric constraints. As with most nonlinear problems, the resulting problem does not have closed-form solutions. The full problem is solved by a Legendre pseudospectral method implemented in DIDO. DIDO exploits SNOPT, an active-set sequential quadratic programming solver, and generates quick solutions to facilitate redesign, an important requirement during the early stages of formation design. This approach does not use linearizations in modeling the dynamics, nor does it require analytical results; rather, the inherent nonlinearities associated with the problem are automatically exploited. Furthermore, we take advantage of a true distributed system architecture that does not rely on designing a leader–follower system. Sample results for formations about the sun–Earth and Earth–moon $L2$ point in the three-body circular restricted dynamical framework are presented. Optimal solutions for relaxed and almost periodic formations are presented for both a large separation constraint (about a third to half of orbit size), and a small separation constraint (about a millionth of orbit size).

I. Introduction

GIVEN the old adage that two or more persons working cooperatively can achieve more than the sum of their individual efforts, it is no surprise that the same holds for space systems. In fact, this concept holds for many other control systems such as underwater vehicles, mobile robots, and airplanes, and including nonvehicular control systems such as those arising in medicine, economics, and software engineering. Such multi-agent systems require a certain level of abstraction to manage complexity; see Tanner et al [1] for an excellent review of the literature and some recent results along this direction.

A distributed space system (DSS) is a multi-agent control system and has long been recognized [2,3] as a key technology area to enhance the scope of both military [2,4] and civilian [3,5–7] space applications. A particular type of DSS that is challenging to design [2–5] is a collection of spacecraft in formation. There are essentially two broad subproblems associated with this problem. The first subproblem is payload specific but can be roughly categorized as originating from signal processing requirements [2,8]. That is, given two or more spacecraft collecting the same information or pieces of it, how can the signals be combined to generate information that is greater than the sum of its parts? The second subproblem is the arrangement of two or more spacecraft (sensor systems) organized to meet the payload/information requirements [2]. For many missions, a sufficient condition for this arrangement is rigidity of formation; that is, the physical equivalent of a rigid structure as in terrestrially distributed antennas. In principle, a rigid space formation can be achieved easily by dynamic inversion and precision control [9]; however, the propellant consumption for this control scheme would be so extraordinarily expensive that it would lead to the erroneous conclusion that a space formation is not viable from an engineering viewpoint. In recognizing that a rigid formation is not a necessary condition for many signal processing functions, the two subproblems need to be examined concurrently and not separately. This is because signal processing requires information on the location of the distributed sensors but it does not require their locations to be constant in time. Thus, a critical technology requirement is precision navigation (within fractions of the wavelength of interest) and not necessarily precision control. In other words, for many missions, it is sufficient for a DSS to be a loose collective [10,11]. As described in Sec. II and elsewhere [9,12,13], these payload-specific requirements can be described in terms of state variable constraints. In any event, given these payload-specific constraints and the overwhelming requirement of meeting these constraints with minimum fuel, it becomes necessary to explore a greater number of allowable formation configurations and possibly reevaluate payload/aperture requirements such as fill factor, exposure times, and so on [8]. In other words, for a DSS to be viable it is imperative to concurrently

Presented as Paper 4786 at the AIAA Guidance, Navigation, and Control Conference and Exhibit, Providence, RI, 16–19 August 2004; received 7 July 2005; revision received 10 February 2006; accepted for publication 10 February 2006.

*Graduate Student. Student Member AIAA.
†Research Assistant, LCDR, U.S. Navy. Student Member AIAA.
‡Professor.
§Professor. Associate Fellow AIAA.

design the formation and the minimum-fuel control [12,13]. Thus, we do not necessarily propose to control a predefined formation configuration in minimum fuel (i.e., the problem of optimal formation keeping [14,15]); rather, we follow Ross et al [9,12] and King [13], and propose that the more fundamental problem is to systematically explore constrained formation configurations that are minimum-fuel solutions to reasonably high fidelity models (e.g., nonlinear). Thus, it is part of the method to find several locally optimal solutions, rather than search for the one local optimal solution closest to an estimate of a particular formation configuration. This process opens up the design space to various configurations and paths hitherto unavailable. It is particularly useful in the preliminary design stage of missions wherein the thinking may be restricted to a particular type of control or orbit by presupposing a particular configuration. Our proposed framework allows the possibility of new mission designs by not separating the design problem from the control problem. Once this preliminary concurrent problem is solved, the next step would be to evaluate the formation configurations for science or military applications, modify the requirements if necessary (by adding suitable constraints), re-solve the problem and reevaluate the result in conjunction with the propellant expenditures to determine its viability [12]. This approach of telling agents what to do, rather than how to do it ("meta-control"), has been successfully applied for the design and control of a variety of Earth-orbiting formations [12,13], station-keeping of libration-point missions [16], multisatellite trajectory optimization [17], and multi-agent mission planning [18]. In this paper, we extend the results of Infeld and Murray [16] by adopting the approach of Ross and King [9,12,13].

Similar to the extensive work on spacecraft formation in the two-body problem, much of the research on the three-plus-body problem is centered around linearization about a reference libration orbit [19–22]. That is, the problem is split into two subproblems: the design of a "good" reference orbit and formation control around the reference orbit. Note that this splitting of the problems is not the same as the splitting of the design and control problems noted earlier; these are additional simplifications that are easily circumvented by the ideas promulgated in Sec. IV. In addition, as explained in Sec. III, these premature simplifications generate harder subproblems. Nonetheless, whereas such a two-step approach may be viable for certain missions, a simple, unified, single-step approach can be articulated as proposed by Ross and King [9,12,13]. In this approach, the orbits and the formation control strategies are designed concurrently using the framework of multi-agent optimal control theory [18]. It will be apparent shortly that this framework, described in Sec. II, is not the same as applying optimization techniques to compute the standard problem of impulsive trajectory correction maneuvers [23]. The concurrent approach allows the mission design to be grasped as one problem with greater simplicity while allowing a wider exploration of the trade space in the preliminary design process.

II. General Framework

A general framework for spacecraft formation design and control is described by Ross et al [9,12] and summarized here for the purposes of completeness and clarity. Suppose that we have a collection of $N_s \in \mathbb{N}$ spacecraft that constitute a DSS. Let $\mathbf{x}^i(t) \in \mathbb{R}^{N_{x^i}}$ denote the state of the ith spacecraft at time t. This can be the usual six-vector position-velocity state or any other set (e.g., orbital elements). We assume that the dynamics of the DSS is given in some coordinate system by a set of differential equations,

$$\dot{\mathbf{x}}^i = \mathbf{f}^i(\mathbf{x}^i, \mathbf{u}^i, t; \mathbf{p}^i) \qquad i = 1 \ldots N_s \tag{1}$$

where $\mathbf{f}^i$: $\mathbb{R}^{N_{x^i}} \times \mathbb{R}^{N_{u^i}} \times \mathbb{R} \times \mathbb{R}^{N_{p^i}} \to \mathbb{R}^{N_{x^i}}$ is a given function, $\mathbf{u}^i \in \mathbb{U}^i \subseteq \mathbb{R}^{N_{u^i}}$ is the control variable of the ith spacecraft constrained to some compact set $\mathbb{U}^i$, and $\mathbf{p}^i \in \mathbb{R}^{N_{p^i}}$ is a vector of (constant) design parameters. In general, the dynamics need not be given in state-space form, as in Eq. (1), but for the purpose of brevity we limit our discussion to such a vector-field approach. For alternative dynamical descriptions, see [24,25] wherein normal forms, differential inclusions, and flatness parameterizations are exploited. By defining the state and control variables as

$$\mathbf{x} = (\mathbf{x}^1, \ldots, \mathbf{x}^{N_s}) \tag{2}$$

$$\mathbf{u} = (\mathbf{u}^1, \ldots, \mathbf{u}^{N_s}) \tag{3}$$

the dynamics of the DSS may be represented quite succinctly as

$$\dot{\mathbf{x}} = \mathbf{f}(\mathbf{x}, \mathbf{u}, t; \mathbf{p}) \qquad \mathbf{u} \in \mathbb{U} \tag{4}$$

where $\mathbb{U} = \mathbb{U}^1 \times \ldots \times \mathbb{U}^{N_s}$. Typically, the functions $\mathbf{f}^i$ are all the same so that $\mathbf{f}$ is simply N_s copies of $\mathbf{f}^1$. Let $d(\mathbf{x}^i, \mathbf{x}^j) \in \mathbb{R}_+$ be a generic distance metric (not necessarily Euclidean) between any two spacecraft. If $d[\mathbf{x}^i(t), \mathbf{x}^j(t)]$ is a given constant in time, $c^{i,j}$, then we say we have a *frozen formation*,

$$c^{i,j} \le d[\mathbf{x}^i(t), \mathbf{x}^j(t)] \le c^{i,j} \quad \forall\ t, i, j \tag{5}$$

Here and the rest of the paper, by $\forall\ t$, we mean for all t associated with the finite lifetime of the DSS whereas by $\forall\ i, j$ we mean $\forall\ i, j \in \{1, \ldots, N_s\}$. Further, from the definition of a metric, $d(\mathbf{x}^i, \mathbf{x}^j) = 0\ \forall\ i = j$; hence, we must have $c^{i,j} = 0\ \forall\ i = j$ as a necessary condition for feasibility. Note that Eq. (5) is really an equality; the reason for masquerading it as an inequality is to define a *relaxed formation* as

$$c^{i,j} - \delta_l^{i,j} \le d[\mathbf{x}^i(t), \mathbf{x}^j(t)] \le c^{i,j} + \delta_u^{i,j} \quad \forall\ t, i, j \tag{6}$$

where $\delta_l^{i,j} \ge 0$ and $\delta_u^{i,j} \ge 0$ are lower and upper tolerances associated with the relaxation. When $i = j$, the tolerances must be zero in conformance with the definition of a metric. Equation (6) generalizes Eq. (5) because if $\delta_l^{i,j} = \delta_u^{i,j} = 0\ \forall\ i, j$, we recover the representation of the frozen formation defined by Eq. (5). As suggested in Sec. I, $\delta_l^{i,j}$ is a formation design parameter that can be tied to signal processing requirements. Thus, for different missions and different portions of the electromagnetic spectrum, $\delta_l^{i,j}$ may be substantially different. Nonetheless, the basic concept captured by Eq. (6) remains valid.

We can define and design various configurations based on a variety of additional requirements. For example, in libration-point missions, to generate halo orbits, there may be a forbidden zone such as a disk of radius R centered around the libration point, $\mathbf{y}$; in this case, we define an allowable region for $\mathbf{x}$ as

$$d[\mathbf{x}^i(t), \mathbf{y}] \ge R \quad \forall\ i, t$$

See King [13] for an implementation of such constraints for a variety of Earth-orbiting missions, such as projected circular formations and natural formations. The requirement that no two spacecraft collide may be articulated as

$$d[\mathbf{x}^i(t), \mathbf{x}^j(t)] \ge b^{i,j} > 0 \quad \forall\ t \text{ and } i \ne j$$

It is apparent that all these constraints (and many more that are specific to a particular mission) can be described in terms of a generic set of a possibly large number of inequality constraints that can be represented as

$$\mathbf{h}^L \le \mathbf{h}(\mathbf{x}, \mathbf{u}, t; \mathbf{p}) \le \mathbf{h}^U \tag{7}$$

where $\mathbf{h}$: $\mathbb{R}^{N_x} \times \mathbb{R}^{N_u} \times \mathbb{R} \times \mathbb{R}^{N_p} \to \mathbb{R}^{N_h}$ and $\mathbf{h}^L, \mathbf{h}^U, \in \mathbb{R}^{N_h}$. In this description of a formation, there is no leader or follower, rather a system of multiple spacecraft. Thus, if any one spacecraft has an additional configuration constraint, it would automatically transfer in some fashion to the remainder of DSS by way of the couplings between the various equations. For example, if there is a mission requirement to designate a particular spacecraft as a leader and designate the others as followers, this can be easily accomplished by picking out the particular index, i, representing the leader. Then, when the leader moves along some trajectory, $t \mapsto \mathbf{x}^i$, the distance metrics along with any additional path constraints, Eq. (7), dictate how the remainder of the spacecraft must follow certain trajectories

to meet the path constraints, i.e., a formation. Thus, although our framework is based on a collection of DSS, it does not exclude a leader–follower system.

As noted earlier, fuel consumption dominates any DSS design. The popular quadratic cost functions are inappropriate measures of fuel [26] and hence we limit our attention to the l^p family of L^1-norms [9]. More specifically, we limit our attention to the l^1-variant of the L^1 norm of control, which represents a practical configuration of six thrusters. Then, the fuel consumption for any one spacecraft, i, is given by

$$J_i = \int_{t_0}^{t_f} \|\mathbf{u}^i(t)\|_1 \mathrm{d}t \tag{8}$$

where $t_f - t_0$ is the time interval of interest and $\|\cdot\|_1$ is the usual l^1-norm. Note that this cost function is nonsmooth [27]. Nonetheless, the discretized system is a well-posed, smooth problem as a result of transformations. See [26] for further discussions of the issues of norms in cost functions involving thrusters and the resulting discretized system. Treating the problem to be invariant under time translations allows us to set $t_0 = 0$. A critical modeling issue in the design and control of spacecraft formations is the treatment of the horizon, t_f, vis-à-vis the mission life time. Ideally, we would like to choose t_f to be equal to the mission life. Deferring a discussion of alternative choices for the horizon, we choose the cost functional for designing the DSS to be the total fuel consumption,

$$J = \sum_{i=1}^{N_s} J_i = \int_{t_0}^{t_f} \sum_{i=1}^{N_s} \|\mathbf{u}^i(t)\|_1 \mathrm{d}t \tag{9}$$

In certain applications, it may be necessary to require that each spacecraft in the DSS consume the same amount of propellant. This requirement can be stipulated by the so-called isoperimetric constraints,

$$J_i = J_k \quad \forall\ i, k \tag{10}$$

If the equal-fuel requirement is "soft" as in $J_i \approx J_k$, it can be simply stipulated as an inequality with appropriate upper and lower bounds. Likewise, the allocation of fuel budgets can be similarly defined.

It will be apparent shortly that the problem formulation as posed so far is quite sufficient to handle libration-point formations in the sun–Earth system if the spacecraft lifetime measured in terms of the duration of the formation is about a year or so as in the Genesis mission [28]. This is because the number of halo orbits over this duration is about two. For a similar lifespan, the number of orbits in the two-body Earth system range from several hundred to thousands. We can take advantage of the smaller ratio of "natural orbit" period to mission lifetime by forming the design problem to create one optimal orbit. If this orbit is required to be almost periodic, the trajectory and control can be assumed to continue for the few more orbits necessary to complete the mission lifetime with the same controls and therefore same fuel cost. We choose this practical problem formulation for some further examples of the application of the concurrent design approach.

By adapting Bohr's notion of almost periodic functions [29,30], periodicity may be exploited to create the alternative problem formulation based on a modification to optimal periodic control theory. In this problem formulation, we write [12,31]

$$J = \frac{1}{t_f - t_0} \int_{t_0}^{t_f} \sum_{i=1}^{N_s} \|\mathbf{u}^i(t)\|_1 \mathrm{d}t \tag{11}$$

which is a measure of fuel consumed by the DSS averaged over the time period $(t_f - t_0)$. It is quite tempting to choose a priori this time period equal to the period of some appropriately chosen reference orbit; however, a far better option [12] is to let this period be free so that the problem formulation allows the determination of an optimal time period as well. As noted in Sec. I, this is one of the ways we use meta-control. To facilitate the existence of a solution for this scenario, it is now necessary to impose two additional constraints on the problem formulation:

1) The dynamical equations, Eq. (1), must be written in an appropriate coordinate system that facilitates a periodic or almost periodic solution.

2) Boundary conditions representing the almost periodic structure of the desired solution must be included.

Thus, assuming that the first condition is satisfied, the boundary conditions for strict periodicity of a *periodic formation* can be stipulated as

$$\mathbf{x}^i(t_0) = \mathbf{x}^i(t_f) \quad \forall\ i \tag{12}$$

Two points are worth noting at this juncture: first, these conditions are not the same as specifying standard boundary conditions because the values of $\mathbf{x}^i(t_0)$ and $\mathbf{x}^i(t_f)$ are unknown. Second, as briefly noted earlier, it is sufficient to stipulate all the constraints of Eq. (12) as a single constraint,

$$\mathbf{x}^i(t_0) = \mathbf{x}^i(t_f) \quad \text{for } i = 1 \tag{13}$$

or any other index. This is because the path constraints will automatically enforce the remainder of the periodic constraints for a small formation size relative to the orbit size. In this context, $i = 1$ is the generalized leader in the sense of traditional leader–follower architecture. By relaxing the constraint represented by Eq. (12) to

$$\varepsilon_l^i \le \mathbf{x}^i(t_0) - \mathbf{x}^i(t_f) \le \varepsilon_u^i \quad \forall\ i \tag{14}$$

where ε_l^i and ε_u^i are formation design parameters, we stipulate a practical means to design and control almost periodic formations [13]. It is clear from these definitions that a frozen formation in the Euclidean metric is a periodic formation but not vice versa. The concept of almost periodicity is not only quite practical, it has significant theoretical advantages. See Fischer [29] for a quick review of almost periodic functions, and Junge et al [32] for practical demonstrations of possible contradictions in applying ordinary Floquet analysis. Deferring the details of applying this framework for libration-point missions to Sec. IV, we note that the problem of designing and controlling spacecraft formations can be summarized as a nonsmooth, nonlinear, multi-agent optimal control problem,

$$(B)\begin{cases} \text{Minimize} & J[\mathbf{x}(\cdot), \mathbf{u}(\cdot), t_0, t_f] = \frac{1}{t_f - t_0} \int_{t_0}^{t_f} \sum_{i=1}^{N_s} \|\mathbf{u}^i(t)\|_1 \mathrm{d}t \\ \text{Subject to} & \dot{\mathbf{x}}(t) = \mathbf{f}[\mathbf{x}(t), \mathbf{u}(t), t; \mathbf{p}] \\ & \mathbf{u}(t) \in \mathbb{U}[t, \mathbf{x}(t), \mathbf{p}] \\ & [\mathbf{x}(t_0), \mathbf{x}(t_f), t_0, t_f] \in \mathbb{E} \end{cases}$$

where $\mathbb{U}$ is written in a form to indicate state-dependent control constraints as in Eq. (7), and $\mathbb{E}$ represents generic endpoint conditions of the form given by Eq. (14).

III. Solving General Formation Problems

It is thus clear that solving a generic formation problem is tantamount to solving a state-constrained optimal control problem. Because solving optimal control problems, particularly state-constrained problems, are widely considered to be difficult [33,34], it is natural to conclude that formation problems are also difficult problems. Over the last decade, there has been a substantial rethinking in classifying hard and easy optimal control problem. For example, Rockafellar [35] notes that it is nonconvexity, not nonlinearity, that makes an optimization problem hard. More recently, Hager [36] showed that standard "convergent" Runge–Kutta (RK) methods fail to converge for optimal control problems. In other words, if one uses a standard RK method to discretize an optimal control problem and if the resulting finite dimensional optimization problem is convex, it will appear very easy to solve but will generate the wrong answer! To add to this apparent confusion, Betts et al [37] showed that "nonconvergent" RK methods converge. Note that these issues are markedly different from the difficulties in solving optimal control problems observed in the 1960s [38]. As a

result of such long perceived difficulties, the formation design and control problem has been split into simpler problems as observed in Sec. I. This naturally leads one to the path of ad hoc techniques. Whereas ad hoc techniques may have utility, they lead to an incorrect assessment of the viability of achieving a DSS to meet payload requirements. For example, in a standard procedure, a libration-point formation design is synthesized by designing formation-keeping maneuvers around a reference orbit. The reference orbit is obtained by some version of the Lindstedt–Poincaré approximation technique proposed by Richardson [39]. The accuracy of this method is then judged by comparing the results to a direct numerical integration of the dynamical equations. This naturally leads to a procedure for improving the initial conditions by shooting methods [32,40]. Given the issues raised by Hager [36], it is clear that difficulties will be encountered even when convergent RK methods are used. This is in fact borne out by the research of Junge et al [32], who describe the difficulties of this approach. Thus, an instability of a halo orbit is compounded by numerical instabilities. In addition, when formation-keeping methodologies are developed by applying linear control theory to the linearized equations of motion for a neighboring orbit [21,22,41–44], excessive fuel estimates are obtained, thereby implying that a formation around the reference orbit is not viable. Whereas this problem can be alleviated by developing optimal formation control [45] strategies, the framework of Sec. II suggests that both the reference orbit design and the formation-keeping control be solved in one stroke, and that this combined problem is in fact easier than the two subproblems promulgated in the literature. The origin of this claim (demonstrated in the next section) is centered around recent results in optimal control theory [34,36,37,46], which, among other things, explains how to circumvent the difficulties associated with Hamiltonian systems. For example, if a shooting method is used to find, or tune, a reference orbit and if the integration scheme does not satisfy the symplectic conditions of Hager [36], the integration will diverge even if the physical solution is stable. Much of these technical issues pertaining to solving optimal control problems can be encapsulated by the diagram shown in Fig. 1. Here, Problem B^{λ} represents the primal-dual boundary value problem obtained by applying the minimum principle to Problem B. Much of the difficulties reported in the literature center around solving Problem B^{λ}. Regardless of the type of method applied to solving Problem B^{λ}, the sheer act of using a computer to solve it implies discretization: this is denoted abstractly as Problem $B^{\lambda N}$ to denote that a computational solution is sought after dualization, where N denotes some degree of approximation. Problem $B^{\lambda N}$ is a symplectic boundary value problem, which causes substantial difficulties in numerical propagation [38]. The simpler path to solve optimal controls problems is to discretize first (Problem B^{N} in Fig. 1) and dualize afterwards [46,47]. Solving an optimal control problem is fundamentally different from numerical propagation of an ordinary differential equation: the former is a global problem whereas the latter is local problem. Even traditional methods for convergence analysis must be abandoned in favor of new ideas [37,48]. The implementation of these ideas require that any gap (see Fig. 1) resulting in favor of discretizing before dualizing must be closed, if it can be closed at all. Thus, if integration based on the popular family of Runge–Kutta methods is desired, the correct approach for solving

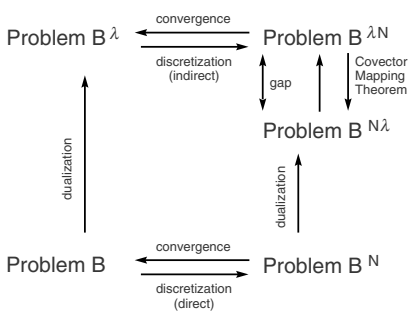

Fig. 1 Covector mapping principle for solving optimal control problems (from Ross and Fahroo [68,69]).

optimal control problems is the Hager family of Runge–Kutta methods [36,48]. By employing the Hager–Runge–Kutta method, convergence of the solution is guaranteed (under appropriate technical conditions). When this concept is combined with a globally convergent algorithm, it is apparent that we can generate solutions using starting points that are not close to a solution. Indeed it may be preferable to use such a starting point because it avoids preconceptions of what are solutions. Globally convergent algorithms have indeed been developed by Gill et al [49] and others [47,50]; thus, a proper blending of new results with such algorithms can be used to solve Problem B.

In this paper we use pseudospectral (PS) methods [51–53]. PS methods have been extremely successful in solving optimal control problems; see the recent paper by Ross and Fahroo [54] and the references contained therein. As a result of its wide success, the next generation of the OTIS software package [55] will have the Legendre PS method as a problem solving option. Further details on NASA's plans are described at: http://trajectory.grc.nasa.gov/projects/lowthrust.shtml. The reason PS methods have been so successful is because they naturally satisfy conditions similar to those of the Hager–Runge–Kutta methods, and offer substantially higher accuracy known as spectral accuracy [53]. Because formation problems can quickly become large scale, the higher accuracy offered by PS methods tempers the growth of the problem in a manner that lends itself to fast solutions on ordinary computers. The origin of this higher accuracy comes from a simple fact that the setting of both optimal control theory and PS methods is a Sobolev space [56]. See Ross [26] for a practical demonstration of the utility of Sobolev spaces. A Sobolev space, denoted as $W^{m,p}(\Omega, \mathbb{R})$, consists of all functions, $f\colon \mathbb{R} \supseteq \Omega \to \mathbb{R}$ whose jth-derivative is in L^p for all $0 \leq j \leq m$. The Sobolev norm of f is defined as

$$\|f\|_{W^{m,p}} := \sum_{j=0}^{m} \|f^{(j)}\|_{L^p} \tag{15}$$

This definition implies that the normed space, $W^{0,p}$, is the same as L^p. The integer m is essentially a mathematical representation of smoothness, as its value is the degree of the derivatives that are continuous and bounded. This concept allows us to state the following informal theorem :

Theorem 1.1 (Convergence) Let $\mathbf{x}^*(\cdot) \in W^{m_x,\infty}([\tau_0, \tau_f], \mathbb{R}^{N_x})$ be the optimal state trajectory associated with the optimal control trajectory, $\mathbf{u}^*(\cdot) \in W^{m_u,\infty}([\tau_0, \tau_f], \mathbb{R}^{N_u})$. Under proper technical conditions, the following convergence result holds:

$$\|\mathbf{x}^*(\cdot) - \mathbf{x}^N(\cdot)\|_{L^\infty} = O(N^{-m_x})$$
$$\|\mathbf{u}^*(\cdot) - \mathbf{u}^N(\cdot)\|_{L^\infty} = O(N^{-m_u})$$

From this theorem it is clear that the rate of convergence of the PS solution is proportional to the smoothness of the optimal solution (the smoother the solution, the faster the convergence). In many problems, this convergence rate is so fast that it is possible to generate real-time solutions [24,25,58]. Real-time computation automatically implies a feedback implementation [26]. For orbit control applications [9], the goals of real-time computation can be met if the computation time is significantly less than the orbital period (relative orbit for formation keeping). This is the well-known concept of a sampled-data feedback system. Given that halo orbital periods for the sun–Earth system are about 180 days, if a computational method took as long as 1 day to compute a solution, it would generate 180 samples per orbit. In other words, solutions obtained in a matter of hours can also be interpreted as a one-sample feedback solution. Thus, the central question now remains: will all these ideas work for the libration-point formation design and control problem?

IV. Libration-Point Formations

In this section, we develop the formation design and control problem under the framework put forth in Sec. II. To this end, let

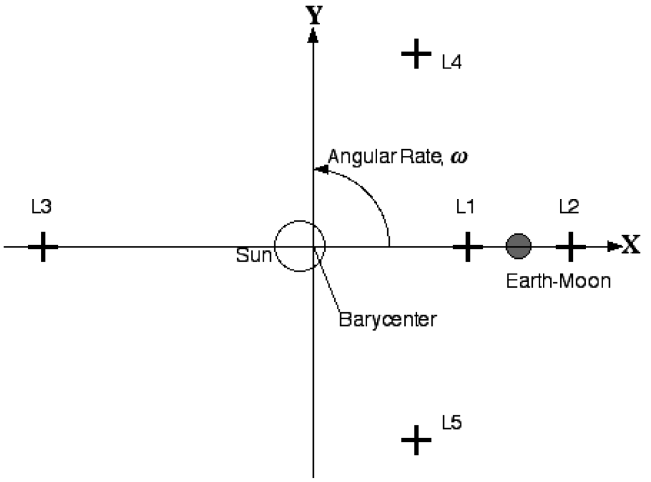

Fig. 2 Coordinate system for the restricted three-body problem.

$\mathbf{r}^i = (x^i, y^i, z^i)$ denote the Cartesian components of a generic spacecraft in the rotating barycentric frame (see Fig. 2) of the circular restricted three-body problem. The spacecraft dynamical equations are well known and given by,

$$\dot{\mathbf{r}}^i = \mathbf{v}^i \tag{16}$$

$$\dot{\mathbf{v}}^i = \mathbf{C}\mathbf{v}^i + \frac{\partial U^i}{\partial \mathbf{r}^i} + \mathbf{u}^i \tag{17}$$

where

$$\mathbf{C} = \begin{pmatrix} 0 & -2 & 0 \\ 2 & 0 & 0 \end{pmatrix} \qquad U^i \equiv U(x^i, y^i, z^i)$$

$$U(x, y, z) = \frac{x^2 + y^2}{2} + \frac{1-\mu}{r_A(x, y, z)} + \frac{\mu}{r_B(x, y, z)}$$

$$r_A^2(x, y, z) = (x + \mu)^2 + y^2 + z^2$$

$$r_B^2(x, y, z) = (x + \mu - 1)^2 + y^2 + z^2$$

The acceleration control $\mathbf{u}^i$ is norm-bounded,

$$\|\mathbf{u}^i\|_\infty \le u^i_{\max}$$

and represents the thruster size of a particular configuration [26]. A multitude of formation options can be defined in various ways. For example, it may be necessary to keep the relative Euclidean distance (l^2-norm) bounded according to

$$c_2^{i,j} - \delta_l^{i,j} \le \|\mathbf{r}^i(t) - \mathbf{r}^j(t)\|_2 \le c_2^{i,j} + \delta_u^{i,j} \quad \forall\ t, i, j \tag{18}$$

Another option may require to bound the l^∞-norm

$$c_\infty^{i,j} - \delta_l^{i,j} \le \|\mathbf{r}^i(t) - \mathbf{r}^j(t)\|_\infty \le c_\infty^{i,j} + \delta_u^{i,j} \quad \forall\ t, i, j \tag{19}$$

as an alternative or additional requirement. In some complex mission geometries, metrics not based on norms may also be used. All the preceding conditions apply to relative formation configurations. To design the ensemble about a generic Lagrange point, $L \in \{L1, \ldots, L5\}$, an allowable zone can be defined as

$$c_l^{i,L} \le \|\mathbf{r}^i(t) - \mathbf{r}_L\|_2 \le c_u^{i,L} \quad \forall\ t, i$$

where $\mathbf{r}_L$ is the position vector of L. Similar to the relative configuration metrics, other metrics or norms may also be chosen for the allowable zone.

All of the preceding conditions apply to a design of the full formation system without requiring leader–follower architecture. As noted before, it is possible to transmit conditions to the entire system by stipulating conditions on any one spacecraft. For example, to create a formation along a halo orbit, it is sufficient to specify the "halo conditions" for just one spacecraft. This is also an orbit design problem and can be designed concurrently with the formation by imposing additional conditions. For example, if the formation system is required to be periodic, then it is sufficient to impose the periodic conditions for just one spacecraft, say

$$\mathbf{r}^j(t_0) = \mathbf{r}^j(t_f) \tag{20}$$

$$\mathbf{v}^j(t_0) = \mathbf{v}^j(t_f) \quad \text{for } j = 1 \tag{21}$$

To generate almost periodic trajectories, these conditions can be relaxed to give

$$\varepsilon_{r,l}^j \le \mathbf{r}^j(t_0) - \mathbf{r}^j(t_f) \le \varepsilon_{r,u}^j \tag{22}$$

$$\varepsilon_{v,l}^j \le \mathbf{v}^j(t_0) - \mathbf{v}^j(t_f) \le \varepsilon_{v,u}^j \quad \text{for } j = 1 \tag{23}$$

It is thus clear that our problem formulation is substantially different from the two-step approach that is commonly employed in the literature [59–63].

V. Examples

Having established the formation design and control problem as a state-constrained, multi-agent, L^1-optimal control problem, the necessary conditions for optimality can be derived in a manner analogous to the procedure described in [9,17]. For the purpose of brevity, these conditions are not listed here; however, they have been verified by the covector mapping principle described in Sec. III. The problem posed in Sec. IV is now solved by the method summarized in Sec. III. As indicated there, we prefer to use a PS method due to its high convergence rate. We used the PS method implemented in DIDO [64]. DIDO is available within the MATLAB problem solving environment and is described as a minimalist's approach to solving optimal control problems. No explicit knowledge of PS methods or nonlinear programming techniques is necessary to use DIDO. The software exploits the suite of mathematical programming solvers available through TOMLAB [65]. The default solver in DIDO is SNOPT [49]. In this section, we demonstrate our ideas for a two-spacecraft system ($N_s = 2$).

The solution is often globally optimal as the algorithm finds an approximately "natural" path in the circular restricted three-body model that needs no fuel use to meet the constraints. We show several examples with simple enough constraints that a globally optimal path is feasible, and is therefore found by the algorithm. When this is not possible, the controls are nonzero, and the solution is a locally optimal one. The final example shows that with periodicity constraints, and by extension, other more strict constraints, the approach will still yield optimal designs that are not restricted to the natural paths as a reference (and so must give lower cost results).

The extension of this approach to three or more spacecraft is straightforward [17], and requires the input of more variables, equations of motion, and constraints to specify the desired relationship of the spacecraft. The increase in computation time is modest because the degrees of freedom of the problem increase at a modest rate as a consequence of additional variables being largely offset by an increase in the number of constraints. Additional details are described in [66].

A. Sun–Earth System

Although our method can be applied to any libration-point mission, we choose to design and control formations about the $L2$ point because of the multitude of telescope formation missions proposed at this location. This gives us the values for μ, the fractional mass (smaller body's mass divided by total system mass), and $\mathbf{r}_L$, the position of the $L2$ point as

$$\mu = 2.448 \times 10^{-6} \qquad \mathbf{r}_L = (1 - \mu + 0.01, 0, 0)\ \text{DU}$$

in the barycentric frame, where DU is the distance unit equal to the

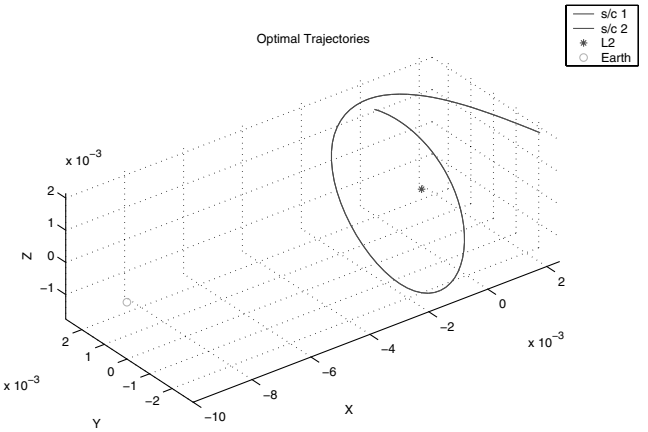

Fig. 3 Optimal formation trajectory design for a two-satellite system.

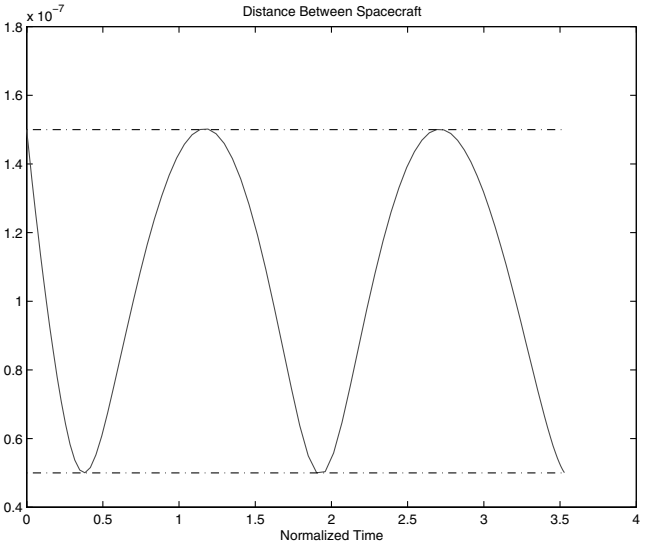

Fig. 4 Separation profile between the two spacecraft of Example 1.

astronomical unit, AU. For computational purposes, the origin is shifted to $L2$ to improve variable scaling. Also, we choose the Euclidean distance, the maximum acceleration and the allowable zone parameters as the design parameters. The separation parameters between the two spacecraft are chosen to reflect the spread of an interferometry mission. For example, for the Terrestrial Planet Finder mission, the requirement is a 1 km range (additional requirements are described in [6]). The next generation of "hypertelescopes" being explored by optical engineers [67] will use much larger baselines for resolution of smaller objects. For example, to observe the characteristics of Earth-sized planets several parsecs away, a 150 km baseline is required. At one million km, the hypertelescope will angularly resolve neutron stars, which are hundreds of parsecs away. We choose 15 km as the separation for our first two examples. This distance is quite small in comparison to the state variable size (four orders of magnitude difference); hence, scaling issues must be resolved to obtain optimal solutions. In the last example, the separation is much larger, approaching one million km, which reflects the design of a constellation of observers, similar to the Solar Wind Satellite proposal,[‖] or the outer edges of the DSS neutron star observer of the distant future.

1. *Example 1: Fixed-Horizon Relaxed Formation*

In the first example, we consider a fixed-horizon problem, and set $t_f = 3.5$ time units (TU) (about 205 days). The time unit is equal to the period of the rotation system, which is the inverse of the frequency (2π rad per year). In seeking a relaxed formation with a separation of 1×10^{-7} DU (about 15 km), we set the design parameters as

$$c_2^{i,j} = 1 \times 10^{-7} \text{ DU} \quad \text{for } i \neq j \tag{24}$$

$$\delta_2^{i,j} = 5 \times 10^{-6} \text{ DU} \quad \text{for } i \neq j \tag{25}$$

$$u_{\max}^{i} = 0.001 \text{ DU/TU}^2 \quad \forall\ i \tag{26}$$

$$J_i = J_k \quad \forall\ i, k \tag{27}$$

Periodic constraints are not imposed but the isoperimetric constraint of equal-fuel consumption is required [cf. Eq. (27)].

The optimized trajectories for this problem for a choice of 100 nodes (roughly, a 99th-order Legendre polynomial) is shown in Fig. 3. The trajectories show that each of the two spacecraft appear to follow the same shaped halolike orbit about $L2$, but parallel along the path, maintaining the tolerances on the specified separation distance as shown in Fig. 4. The optimal controls are all zero and omitted for the purpose of brevity. This occurs because the spacecraft are able to maintain the correct separation while both within a nearly "natural" orbit that requires a negligible amount of thrust to maintain. Thus, this solution is globally optimal because it has zero cost, i.e., $J = 0 \Leftrightarrow \mathbf{u} = \mathbf{0}$.

An independent check on the validity of the solution can be performed by propagating the optimized initial conditions,

$$x^1(t_0) = -0.43 \times 10^{-3}, \qquad v_x^1(t_0) = 2.00 \times 10^{-3}$$
$$y^1(t_0) = 1.52 \times 10^{-3}, \qquad v_y^1(t_0) = -4.30 \times 10^{-3}$$
$$z^1(t_0) = 1.93 \times 10^{-3}, \qquad v_z^1(t_0) = -0.15 \times 10^{-3}$$

Figure 5 shows a comparison of the optimized states to the propagated states of one of the spacecraft wherein the propagation was performed using `ode45` in MATLAB. It is apparent that the propagated states track fairly well to the optimized ones indicating that the 100-node solution is a good solution over this time period for preliminary design considerations. The differences between the optimized and the propagated trajectories decrease with an increase in the number of nodes, thus implying convergence (see Theorem 1.1).

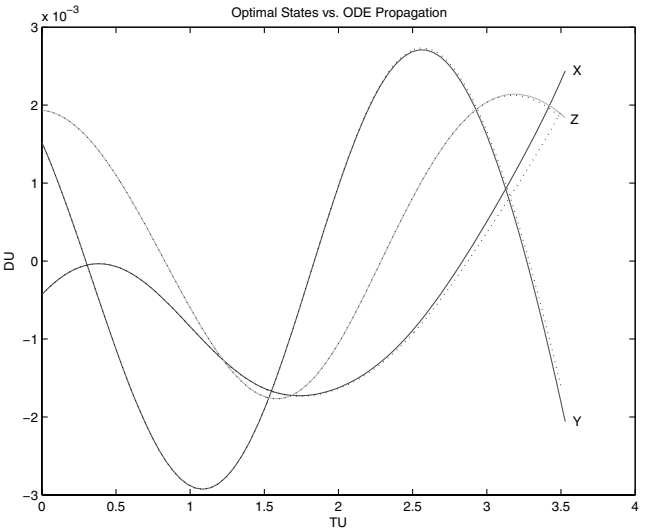

Fig. 5 Comparison of the position states of spacecraft one (solid) to those propagated by `ode45` in MATLAB (dotted).

[‖]Data available online at http://www.wslfweb.org/docs/roadmap/spacroad.htm [cited 23 March 2007].

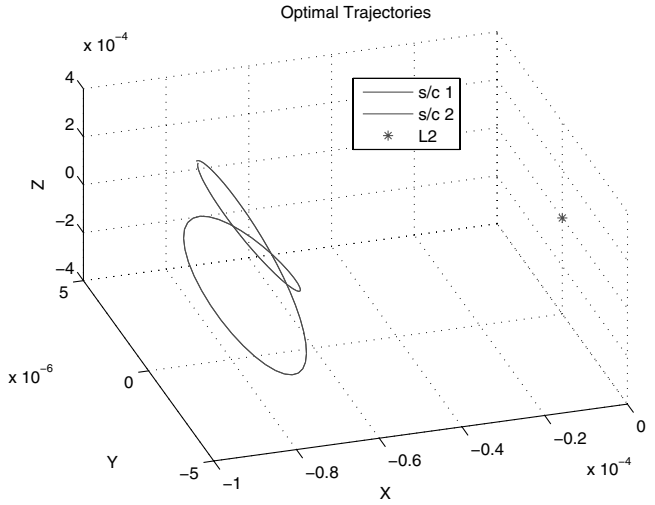

Fig. 6 Optimal trajectories for a two-spacecraft DSS with periodicity constraints. NOT TO SCALE: stretched to show orbit shape.

2. Example 2: Almost Periodic Problem

In this problem, we modify Example 1 by the addition of periodicity constraints. As explained in Sec. II, periodicity in the states is imposed under a free horizon, t_f; thus, we now have,

$$c_2^{i,j} = 1 \times 10^{-7} \text{ DU} \quad \text{for } i \neq j \tag{28}$$

$$\delta_2^{i,j} = 5 \times 10^{-6} \text{ DU} \quad \text{for } i \neq j \tag{29}$$

$$u_{\max}^i = 0.001 \text{ DU/TU}^2 \quad \forall\ i \tag{30}$$

$$J_i = J_k \quad \forall\ i, k \tag{31}$$

$$\mathbf{x}^i(t_0) = \mathbf{x}^i(t_f) \quad \text{for } i = 1 \tag{32}$$

It will be apparent shortly that Eq. (32) will be interpreted in the sense of an almost periodic problem [cf. Eq. (14)]. The optimized trajectories are shown in Fig. 6.

It is immediately apparent that the solution to this problem is substantially different from that of Example 1. The optimal period, t_f, for this design configuration was 3.18 TU, or 185 days. This solution is also globally optimal because $J = 0$. The cost is zero because $\mathbf{u}$ is zero (within numerical tolerances). The trajectories

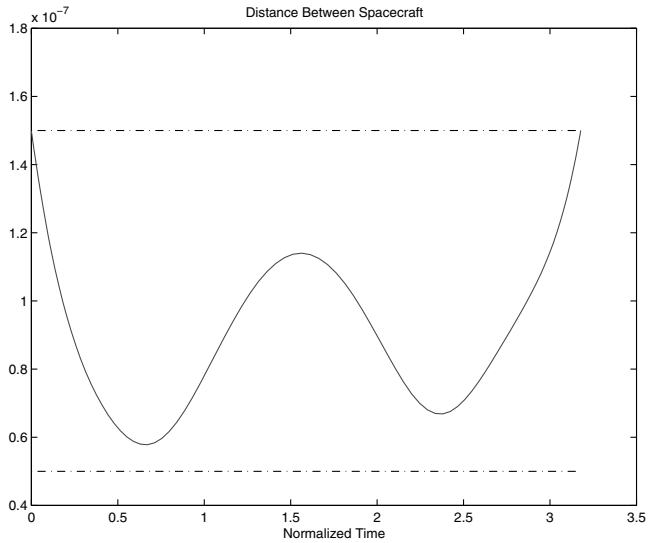

Fig. 7 Separation profile between the two spacecraft of Example 2.

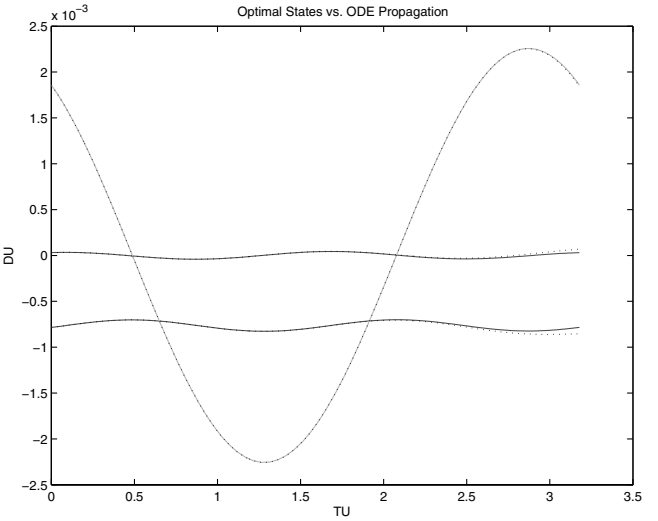

Fig. 8 Comparison of the position states of spacecraft one (solid) to those propagated by `ode45` in MATLAB (dotted).

show that each of the two spacecraft appear to follow the same orbit about $L2$, but parallel along the path, maintaining the tolerances on the specified separation distance as shown in Fig. 7.

As in Example 1, an independent verification of the solution is obtained by propagating a trajectory from the optimized initial conditions (in DU and DU/TU),

$$x^1(t_0) = -0.78 \times 10^{-3}, \qquad v_x^1(t_0) = 0.23 \times 10^{-3}$$
$$y^1(t_0) = 0.03 \times 10^{-3}, \qquad v_y^1(t_0) = 0.05 \times 10^{-3}$$
$$z^1(t_0) = 1.86 \times 10^{-3}, \qquad v_z^1(t_0) = -2.53 \times 10^{-3}$$

Figure 8 shows a comparison of the optimized states to the propagated states of one of the spacecraft. It is apparent that the propagated states track fairly well to the optimized ones indicated that the 100-node solution is a good solution for preliminary design considerations.

3. Example 3: Large Baseline

As mentioned in Sec. I, constellation type missions, like the solar wind system, require large baselines spread out over the libration-point orbital space. In this example, we demonstrate that our approach applies without change to such missions.

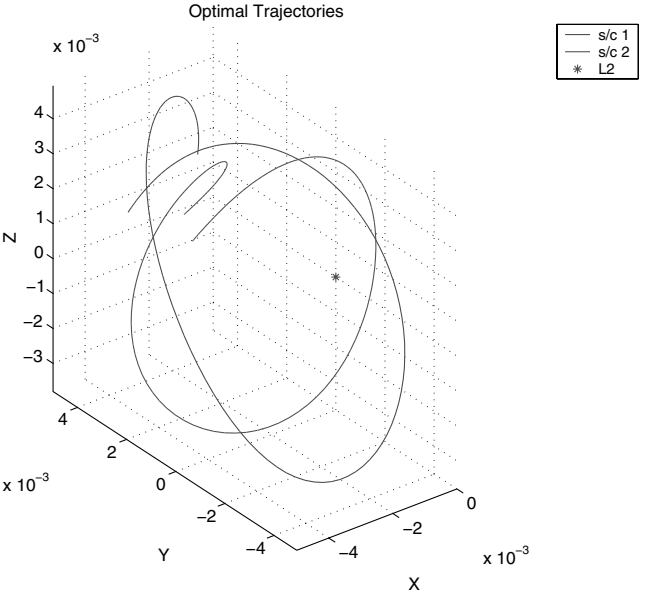

Fig. 9 Optimal trajectories for a large-baseline two-agent DSS.

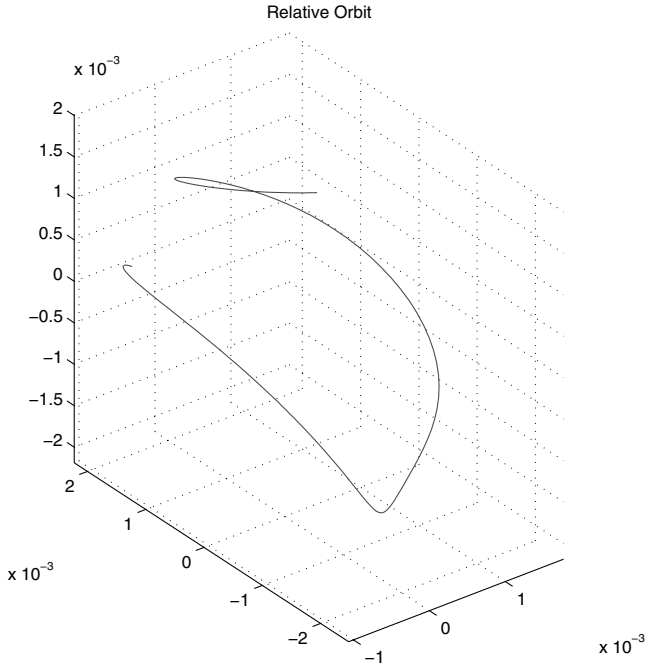

Fig. 10 Relative orbit for the large-baseline two-agent DSS.

The nominal values of the design parameters are

$$c_2^{i,j} = 0.002 \text{ DU} \quad \text{for } i \neq j \tag{33}$$

$$\delta_2^{i,j} = 0.0015 \text{ DU} \quad \text{for } i \neq j \tag{34}$$

$$u_{\max}^{i} = 0.001 \text{ DU/TU} \quad \forall\ i \tag{35}$$

$$t_f = 3.5 \text{ DU} \tag{36}$$

The initial states are all free with no bounds; however, there are bounds on the positions of $\pm 5 \times 10^{-3}$, which is an active constraint at a few time steps for the x-coordinate.

A solution to the problem for the choice of preceding parameters is shown in Fig. 9. This solution again is globally optimal because it has zero cost. The trajectories show that each of the two spacecraft appear to follow distinct halolike orbits about $L2$. The relative orbit is more illustrative of the configuration and is shown in Fig. 10.

Similar to the preceding examples, the convergence of this trajectory can be demonstrated and is not further described here for the purposes of brevity.

B. Earth–Moon System

Potential applications of a DSS in an Earth–moon system are a communications relay for operations on the dark side of the moon and a location of scientific payloads sensitive to Earth-based radio frequency interference (RFI).

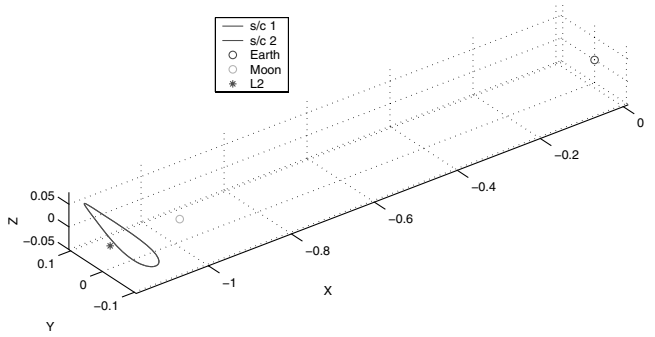

Fig. 11 Optimal trajectories for the Earth–moon periodic $L2$ DSS with 100 km separation (with Earth plotted far right).

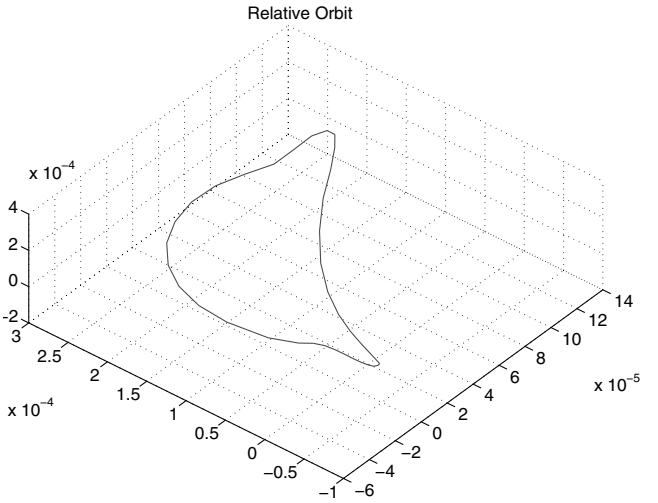

Fig. 12 Relative orbit for the 100 km separation Earth–moon $L2$ solution.

1. *Example 4: Periodic Frozen Formation*

In this example, we again consider a free horizon, periodic, frozen formation, this time with a vehicle separation of 2.6×10^{-6} DU (100 km). However, in this case no isoperimetric constraints are imposed. The other design parameters are

$$c_2^{i,j} = 0.00026 \text{ DU} \quad \text{for } i \neq j \tag{37}$$

$$\delta_2^{i,j} = 0.0000 \text{ DU} \quad \text{for } i \neq j \tag{38}$$

$$u_{\max}^{i} = 0.3381 \text{ DU/TU}^2 \quad \forall\ i \tag{39}$$

The optimized solution is presented in Fig. 11. The trajectories appear to be nearly-identical halo orbits, with an optimal final time of 3.36 TU (approximately 14.6 days). The separation between the spacecraft varies from 2.5991×10^{-004} to 2.6725×10^{-004} DU, a difference of 7.336×10^{-06} DU (slightly more than 2.6 km). The relative motion between the two spacecraft is presented in Fig. 12.

For the purposes of brevity, the tests for convergence and optimality are not reported here but were verified.

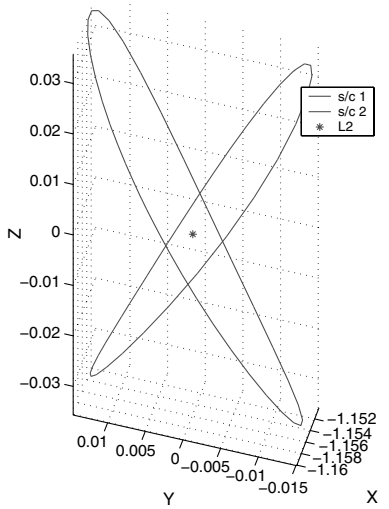

Fig. 13 Optimal trajectories for the Earth–moon periodic $L2$ DSS with 10,000 km separation.

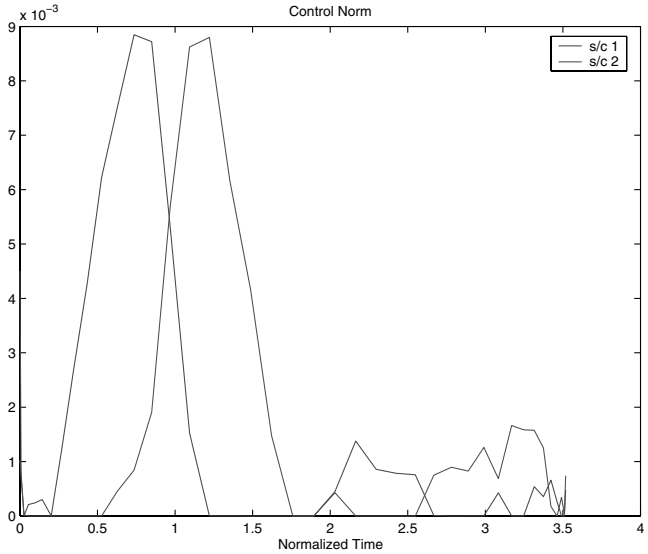

Fig. 14 l^2-norm of controls for the 10,000 km separation, Earth–moon $L2$ solution.

2. Example 5: Large-Baseline Formation

In this final example the problem formation is identical to Example 4, but with an increased spacecraft separation to 0.0260 DU (or 10,000 km). Thus we have

$$c_2^{i,j} = 0.260 \text{ DU} \quad \text{for } i \neq j \tag{40}$$

$$\delta_2^{i,j} = 0.0000 \text{ DU} \quad \text{for } i \neq j \tag{41}$$

$$u_{\max}^{i} = 0.3381 \text{ DU/TU}^2 \quad \forall\ i \tag{42}$$

An optimized solution is presented in Fig. 13. The trajectories are clearly reflections of one another, with an optimal final time, t_f of 3.52 TU (approximately 15.3 days). The controls are small but not zero; see Fig. 14. Thus, this is a locally optimal, but may not be a globally optimal solution. The mean value of 0.0014 DU/TU^2 equates to a mean control acceleration of only 3.7×10^{-6} m/s^2. This control is sufficient to maintain a near-constant separation between the spacecraft as shown in Fig. 15. The separation varies by less 1.5×10^{-6} DU over the trajectory (slightly less than 600 m). The relative motion between the two spacecraft is presented in Fig. 16.

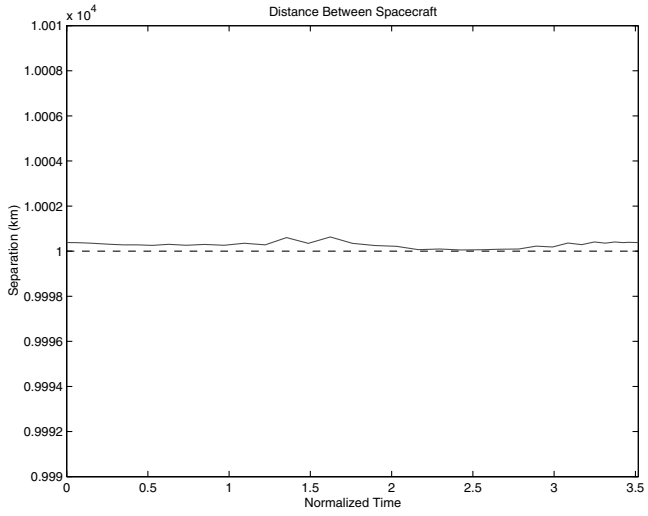

Fig. 15 Separation of the two vehicles over time, 10,000 km Earth–moon solution.

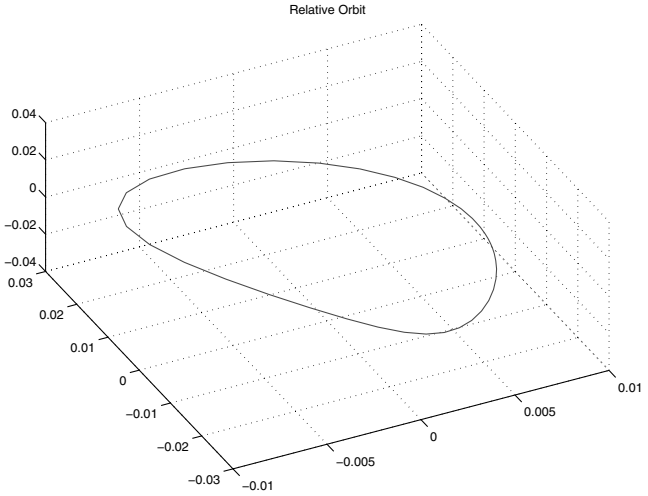

Fig. 16 Relative orbit for the 10,000 km separation Earth–moon $L2$ solution.

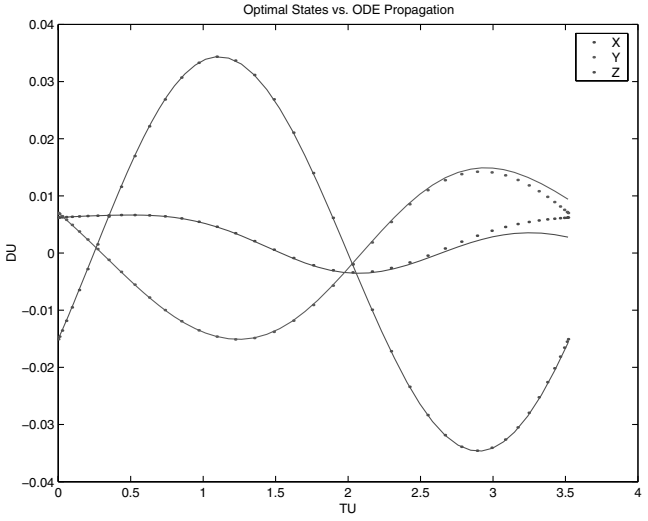

Fig. 17 Comparison of the position states of spacecraft one (dotted) to those propagated by `ode45` using MATLAB (solid) for the 10,000 km separation solution.

The feasibility of this solution is demonstrated by propagating the initial states,

$$x^1(t_0) = -0.0027, \quad x^2(t_0) = 0.0062 \quad y^1(t_0) = 0.0057$$
$$y^2(t_0) = 0.0070 \quad z^1(t_0) = 0.0093, \quad z^2(t_0) = -0.0151$$
$$v_x^1(t_0) = 0.0052, \quad v_x^2(t_0) = 0.0017 \quad v_y^1(t_0) = 0.0258$$
$$v_y^2(t_0) = -0.0213 \quad v_z^1(t_0) = 0.0606, \quad v_z^2(t_0) = 0.0567$$

using interpolated values of the controls. Figure 17 shows some variation between the propagated solution, and the DIDO solution.

VI. Conclusions

To examine the viability of a distributed space system (DSS) to achieve the objective of distributing payload functionality, the formation design and control problem must be solved concurrently. Decoupling the design problem from the control problem not only makes the subproblems harder, but it also restricts the design space to such an extent that erroneous conclusions may be reached. The combined formation design and control problem can be naturally articulated under the general framework of a multi-agent, state-constrained optimal control problem with design parameters. The

difficulties in solving this problem parallel those of solving symplectic boundary value problems. These problems can be overcome by combining recent results from optimal control theory. With the application of these results, the formation design and control problem around a libration point can be solved quickly. Because natural formations are globally fuel-optimal, should the resulting optimal solution require nonzero fuel, the viability of the DSS can be assessed and the design either discarded or the requirements relaxed to explore new solutions.

References

[1] Tanner, H. G., Jadbabaie, A., and Pappas, G. J., "Stable Flocking of Mobile Agents, Part I: Fixed Topology," *Proceedings of the 42nd IEEE Conference on Decision and Control*, Maui, HI, Dec. 2003.

[2] *New World Vistas*, Summary Vol., USAF Scientific Advisory Board, Dec. 1995.

[3] Vincent, M. A., and Bender, P. L., "The Orbital Mechanics of a Space-Borne Gravitational Wave Experiment," *Advances in the Astronautical Sciences, Astrodynamics*, edited by J. K. Soldner, et al., Vol. 65, Pt. II, 1987, p. 1346; also AAS Paper 87-523.

[4] Ross, I. M., "A Mechanism for Precision Orbit Control With Applications to Formation Keeping," *Journal of Guidance, Control, and Dynamics*, Vol. 25, No. 4, 2002, pp. 818–820.

[5] Carpenter, R. J., Leitner, J. A., Folta, D. C., and Burns, R. D., "Benchmark Problems for Spacecraft Formation Flying Missions," AIAA Paper 2003-5364, Aug. 2003.

[6] Lindensmith, C. A. (ed.), "Technology Plan for the Terrestrial Planet Finder," Jet Propulsion Laboratory Publication 03-007, 2003

[7] Fridlund, C. V. M., "Darwin—The Infrared Space Interferometry Mission," *ESA Bulletin*, Vol. 103, Aug. 2000, pp. 20–25.

[8] Fienup, J. R., "MTF and Integration Time Versus Fill Factor for Sparse-Aperture Imaging Systems," Imaging Technology and Telescopes, *Proceedings of the SPIE 4091A-06*, San Diego, CA, July 2000.

[9] Ross, I. M., "Space Trajectory Optimization and L^1-Optimal Control Problems," *Modern Astrodynamics*, Elsevier, New York, 2006 (to appear).

[10] Ramirez, J., and Chakravorty, S., "Fuel Optimal Spiral Maneuvers for Multispacecraft Interferometric Imaging Systems in Deep Space," AAS Paper 06-164, 2006.

[11] Curtis, S., "The Magnetospheric Multiscale Mission ... Resolving Fundamental Processes in Space Plasmas," *Report of the NASA Science and Technology Definition Team for the Magnetospheric Multiscale (MMS) Mission*, NASA TM2000209883, 2000.

[12] Ross, I. M., King, J. T., and Fahroo, F., "Designing Optimal Spacecraft Formations," AIAA Paper 2002-4635, Aug. 2002.

[13] King, J. T., "A Framework for Designing Optimal Spacecraft Formations," M.S. Thesis, Dept. of Aeronautical and Astronautical Engineering, Naval Postgraduate School, Monterey, CA, Sept. 2002.

[14] Campbell, M., "Planning Algorithm for Multiple Satellite Clusters," *Journal of Guidance, Control, and Dynamics*, Vol. 26, No. 5, 2003, pp. 770–780.

[15] Zanon, D., and Campbell, M., "Optimal Planning for Tetrahedral Formations Near Elliptical Orbits," AIAA Paper 2004-5127, Aug. 2004.

[16] Infeld, S. I., and Murray, W., "Optimization of Stationkeeping for a Libration Point Mission," AAS Paper 04-150, Feb. 2004.

[17] Mendy, P. B., "Multiple Satellite Trajectory Optimization," Astronautical Engineer Thesis, Dept. of Mechanical and Astronautical Engineering, Naval Postgraduate School, Monterey, CA, Dec. 2004.

[18] Ross, I. M., and D'Souza, C. D., "Hybrid Optimal Control Framework for Mission Planning," *Journal of Guidance, Control, and Dynamics*, Vol. 28, No. 4, 2005, pp. 686–697.

[19] Marchand, B. G., and Howell, K. C., "Formation Flight Near L_1 and L_2 in the Sun-Earth/Moon Epheremis System Including Solar Radiation Pressure," AAS Paper 03-596, Aug. 2003.

[20] Hsiao, F. Y., and Scheeres, D. J., "Design of Spacecraft Formation Orbits Relative to a Stabilized Trajectory," AAS Paper 03-175, 2003.

[21] Hamilton, N. H., Folta, D., and Carpenter, R., "Formation Flying Satellite Control Around the $L2$ Sun-Earth Libration Point," AIAA Paper 2002-4528, Aug. 2002.

[22] Gurfil, P., and Kasdin, N. J., "Dynamics and Control of Relative Motion in an Unstable Orbit," AIAA Paper 2000-4135, Aug. 2000.

[23] Serban, R., Koon, W. S., Lo, M., Marsden, J. E., Petzold, L. R., Ross, S. D., and Wilson, R. S., "Halo Orbit Mission Correction Maneuvers Using Optimal Control," *Automatica: The Journal of IFAC, the International Federation of Automatic Control*, Vol 38, 2002, pp. 571–583.

[24] Ross, I. M., and Fahroo, F., "A Unified Framework for Real-Time Optimal Control," *Proceedings of the IEEE Conference on Decision and Control*, Maui, HI, Dec. 2003.

[25] Ross, I. M., and Fahroo, F., "Pseudospectral Methods for Optimal Motion Planning of Differentially Flat Systems," *IEEE Transactions on Automatic Control*, Vol. 49, No. 8, 2004, pp. 1410–1413.

[26] Ross, I. M., "How to Find Minimum-Fuel Controllers," AIAA Paper 2004-5346, Aug. 2004.

[27] F. H. Clarke, Y. S. Ladyaev, R. J. Stern, and P. R. Wolenski, *Nonsmooth Analysis and Control Theory*, Springer–Verlag, New York, 1998.

[28] Lo, M., Williams, B. G., Bollman, W. E., Han, D., Hahn, Y., Bell, J. L., Hirst, E. A., Corwin, R. A., Hong, P. E., Howell, K. C., Barden, B., and Wilson, R., "Genesis Mission Design," AIAA Paper 98-4468, 1998.

[29] Fischer, A., "Structure of Fourier Exponents of Almost Periodic Functions and Periodicity of Almost Periodic Functions," *Mathematical Bohemica*, No. 3, 1996, pp. 249–262.

[30] Corduneanu, C., *Almost Periodic Functions*, John Wiley, New York, 1968.

[31] Ross, I. M., Yan, H., and Fahroo, F., "A Curiously Outlandish Problem in Orbital Mechanics," AAS Paper 01-430, July 2001.

[32] Junge, O., Levenhagen, J., Seifried, A., and Dellnitz, M., "Identification of Halo Orbits for Energy Efficient Formation Flying," *Proceedings of the International Symposium on Formation Flying*, Toulouse, France, 2002.

[33] Vinter, R. B., *Optimal Control*, Birkhäuser, Boston, MA, 2000.

[34] Hager, W. W., *Numerical Analysis in Optimal Control*, edited by K.-H. Hoffmann, I. Lasiecka, G. Leugering, J. Sprekels, and F. Troeltzsch, Vol. 139, International Series of Numerical Mathematics, Birkhäuser, Basel, Switzerland, 2001, pp. 83–93.

[35] Rockafellar, R. T., "Lagrange Multipliers and Optimality," *SIAM Review*, Vol. 35, No. 2, 1993, pp. 183–283.

[36] Hager, W. W., "Runge-Kutta Methods in Optimal Control and the Transformed Adjoint System," *Numerische Mathematik*, Vol. 87, No. 2, 2000, pp. 247–282.

[37] Betts, J. T., Biehn, N., and Campbell, S. L., "Convergence of Nonconvergent IRK Discretizations of Optimal Control Problems with State Inequality Constraints," *SIAM Journal on Scientific Computing*, Vol. 23, No. 6, 2002, pp. 1981–2007.

[38] Bryson, A. E., and Ho, Y.-C., *Applied Optimal Control*, Hemisphere, Menlo Park, CA, 1975, Chap. 7.

[39] Richardson, D. L., "Analytic Construction of Periodic Orbits About the Collinear Points," *Celestial Mechanics*, Vol. 22, No. 2, 1980, pp. 241–253.

[40] Kim, M., and Hall, C. D., "Lyapunov and Halo Orbits about L_2," AAS Paper 01-324, 2001.

[41] Carlson, B., Pernicka, H., and Balakrishnan, S., "Spacecraft Formation Flight About Libration Points," AIAA Paper 2004-4737, 2004.

[42] Pernicka, H., Carlson, B., and Balakrishnan, S., "Discrete Maneuver Formationkeeping at Libration Points $L1$ and $L2$," AAS Paper 05-194, Jan. 2005.

[43] McLoughlin, T., and Campbell, M., "Hybrid Leader Follower and Sensor Scheduling for Large Spacecraft Networks," AIAA Paper 2004-5022, 2004.

[44] Gurfil, P., and Kasdin, N. J., "Dynamics and Controls of Spacecraft Formation Flying in Three-Body Trajectories," AIAA Paper 2001-4026, Aug. 2001.

[45] Hussein, I. I., Scheeres, D. J., and Hyland, D. C., "Optimal Formation Control for Imaging and Fuel Usage," AAS Paper 05-160, Jan. 2005.

[46] Ross, I. M., "A Roadmap for Optimal Control: The Right Way to Commute," *Annals of the New York Academy of Sciences*, Vol. 1065, to appear.

[47] Betts, J. T., *Practical Methods for Optimal Control Using Nonlinear Programming*, Advances in Control and Design Series, SIAM, Philadelphia, PA, 2001.

[48] Dontchev, A. L., Hager, W. W., and Veliov, V. M., "Second-Order Runge-Kutta Approximations in Control Constrained Optimal Control Problems," *SIAM Journal on Numerical Analysis*, Vol. 38, No. 1, 2000, pp. 202–226.

[49] Gill, P. E., Murray, W., and Saunders, M. A., "SNOPT: An SQP Algorithm for Large-Scale Constrained Optimization," *SIAM Review*, Vol. 47, No. 1, 2005, pp. 99–131.

[50] Boggs, P. T., and Tolle, J. W., "Sequential Quadratic Programming," *Acta Numerica*, Cambridge Univ. Press, Cambridge, England, U.K., 1995, p. 151.

[51] Canuto, C., Hussaini, M. Y., Quarteroni, A., and Zang, T. A., *Spectral Methods in Fluid Dynamics*, Springer–Verlag, New York, 1988.

[52] Elnagar, J., Kazemi, M. A., and Razzaghi, M., "The Pseudospectral Legendre Method for Discretizing Optimal Control Problems," *IEEE Transactions on Automatic Control*, Vol. 40, No. 10, 1995, pp. 1793–

1796.
[53] Trefethen, L. N., *Spectral Methods in MATLAB*, SIAM, Philadelphia, PA, 2000.
[54] Ross, I. M., and Fahroo, F., "Pseudospectral Knotting Methods for Solving Optimal Control Problems," *Journal of Guidance, Control, and Dynamics*, Vol. 27, No. 3, 2004, pp. 397–405.
[55] Paris, S. W., and Hargraves, C. R., *OTIS 3.0 Manual*, Boeing Space and Defense Group, Seattle, WA, 1996.
[56] Adams, R. A., *Sobolev Spaces*, Academic Press, New York, 1975.
[57] Gong, Q., Ross, I. M., Kang, W., and Fahroo, F., "Convergence of Pseudospectral Methods for Constrained Nonlinear Optimal Control Problems," *Intelligent Systems and Control*, Series on Modelling, Identification and Control, Acta Press, Calgary, Canada, 2004.
[58] Gong, Q., Kang, W., and Ross, I. M., "A Pseudospectral Method for the Optimal Control of Constrained Feedback Linearizable Systems," *IEEE Transactions on Automatic Control*, to appear.
[59] Howell, K. C., and Marchand, B. G., "Design and Control of Formations Near the Libration Points of the Sun-Earth/Moon Ephemeris System," *GSFC Flight Mechanics Symposium*, Greenbelt, MD, Oct. 2003.
[60] Marchand, B. G., and Howell, K. C., "Aspherical Formations near the Libration Points in the Sun-Earth/Moon Ephemeris System," AAS Paper 04-157, Feb. 2004.
[61] Folta, D., Hartman, K., Howell, K., and Marchand, B., "Formation Control of the MAXIM L2 Libration Orbit Mission," AIAA Paper 2004-5211, Aug. 2004.
[62] Howell, K. C., and Marchand, B. G., "Formations Near the Libration Points: Design Strategies Using Natural and Non-Natural Arcs," *GSFC 2nd International Symposium on Formation Flying Missions and Technologies*, Greenbelt, MD, Sept. 2004.
[63] Luquette, R., J., and Sanner, R. M., "A Non-Linear Approach to Spacecraft Formation Control in the Vicinity of a Collinear Libration Point," AAS Paper 01-330, Aug. 2001.
[64] Ross, I. M., and Fahroo, F., "User's Manual for DIDO 2002: A MATLAB Application Package for Dynamic Optimization," Naval Postgraduate School, Dept. of Aeronautics and Astronautics, NPS Technical Report AA-02-002, Monterey, CA, June 2002.
[65] Holmström, K., Göran, A. O., and Edvall, M. M., *User's Guide for Tomlab 4.0.6*, Tomlab Optimization, Sweden, Aug. 2003.
[66] Infeld, S. I., "Optimization of Mission Design for Constrained Libration Point Space Missions," Ph.D. Dissertation, Dept. of Aeronautics and Astronautics, Stanford Univ., Stanford, CA, Jan. 2006.
[67] Labeyrie, A., Le Coroller, H., Dejonghe, J., Martinache, F., Borkowski, V., Lardire, O., and Koechlin, L., "Hypertelescope Imaging: From Exo-Planets to Neutron Stars," *Proceedings of SPIE Conference*, Vol. 4852, Hawaii, 2002.
[68] Ross, I. M., and Fahroo, F., "A Perspective on Methods for Trajectory Optimization," AIAA Paper 2002-4727, Aug. 2002.
[69] Ross, I. M., and Fahroo, F., "Legendre Pseudospectral Approximations of Optimal Control Problems," *Lecture Notes in Control and Information Sciences*, Vol. 295, Springer–Verlag, New York, 2003.